Regular Article

# Enhancing the stability of rotating machinery using a lower pad adjustable journal bearing

Lei Zhang[1,2] · Hua Xu[1,2] · Shenglun Zhang[1,2] · Shiyuan Pei[1,2]



**Abstract**
A lower pad adjustable journal bearing is proposed in this paper. This bearing can adjust the working status of the rotor system by changing the position of the bearing pad and improve the stability of the rotor system. The adjustable bearing structure achieves the function of changing the characteristic parameters of the bearing under continuous operation and makes up for the shortcomings of the traditional fixed-pad bearing. In this paper, the evaluation method of the dynamic characteristics of the adjustable bearing is introduced. The stiffness and damping characteristics of the bearing are calculated by the analytical method. Then, the rotor bearing system model is established using the finite element method. Finally, the dynamic response of the rotor system is solved by Runge–Kutta variable step length integration. The numerical results show that the stability of the system can be improved by reducing the ellipticity of the adjustable bearing when the rotor system crosses the critical speed. The experimental study shows that when the oil film is unstable in the rotor system, the oil film whip is effectively eliminated by reducing the ellipticity, which proves that the adjustable bearing can improve the stability of the rotating machine.

**Keywords** Adjustable bearings · Elliptical · Stiffness and damping coefficient · Rotor dynamics · Oil film instability

**List of symbols**

| | |
|---|---|
| $O$ | Geometric center of bearing |
| $O'$ | Journal center |
| $O_1$ | Lower pad center |
| $O_2$ | Upper pad center |
| $e$ | Journal eccentricity |
| $e_1$ | Distance between center of journal and Center of lower bearing pad |
| $e_2$ | Distance between center of journal and Center of upper bearing pad |
| $\theta$ | Attitude angle of journal |
| $\theta_1$ | Attitude angle of lower pad |
| $\theta_2$ | Attitude angle of upper pad |
| $W$ | Bearing load |
| $R$ | Bearing radius |
| $r$ | Journal radius |
| $h$ | Film thickness of elliptical bearing |
| $c_r$ | Radius clearance |
| $c_{max}$ | Side clearance |
| $c_{min}$ | Top clearance |
| $l$ | Bearing width |
| $d$ | Bearing diameter |
| $\lambda$ | Coordinate at the axial direction of the bearing |
| $\delta$ | Elliptical ratio/ellipticity |
| $\varepsilon$ | Journal relative eccentricity, $\varepsilon = \frac{e}{c_r}$ |
| $e'$ | Distance between center of bearing and center of bearing pad |
| $\varphi$ | Angular coordinate of adjustable bearing |
| $P$ | Oil film pressure of adjustable bearing |
| $P_e$ | The derivative of oil film pressure to displacement disturbance of $e$ |
| $P_\theta$ | The derivative of oil film pressure to displacement disturbance of $\theta$ |

✉ Lei Zhang, leizhang2018@vt.edu; ✉ Hua Xu, xuhua@mail.xjtu.edu.cn | [1]School of Mechanical Engineering, Xi'an Jiaotong University, Xi'an 710049, People's Republic of China. [2]Key Laboratory of Education Ministry for Modern Design and Rotor-Bearing System, Xi'an Jiaotong University, Xi'an 710049, People's Republic of China.

SN Applied Sciences (2019) 1:420 | https://doi.org/10.1007/s42452-019-0419-2

Received: 14 February 2019 / Accepted: 26 March 2019 / Published online: 5 April 2019

| | |
|---|---|
| $P_{\dot{e}}$ | The derivative of oil film pressure to the velocity disturbance of $\dot{e}$ |
| $P_{\dot{\theta}}$ | The derivative of oil film pressure to the velocity disturbance of $\dot{\theta}$ |
| $\varphi_1$ | Angular coordinate of lower bearing pad |
| $\varphi_2$ | Angular coordinate of upper bearing pad |
| $\varphi_{11}$ | The angle of the beginning of the lower pad oil film |
| $\varphi_{12}$ | The angle of the end of the lower pad oil film |
| $\varphi_{21}$ | The angle of the beginning of the upper pad oil film |
| $\varphi_{22}$ | The angle of the end of the upper pad oil film |
| $K_{xx}$, $K_{xy}$, $K_{yx}$, $K_{yy}$ | Stiffness coefficients |
| $D_{xx}$, $D_{xy}$, $D_{yx}$, $D_{yy}$ | Damping coefficients |

## 1 Introduction

The development of rotating machinery for high speed, heavy load and automation, place higher requirements on the operational stability and safety of the rotating machinery. The traditional rotating machinery is generally supported by fixed-pad bearings. When the rotating machinery is unstable due to the change, in rotational speed and load, the fixed-pad bearing cannot adjust to the different working conditions, nor can it improve the running status of the rotating machinery. The rotating machinery, supported by the fixed-pad bearing, is designed based on a specific working condition. In the actual operation process, its working condition may change. The initial design state and actual working state of the rotor bearing system may be different. For example, the generator set will adjust its working load according to the difference in power consumption; the operating speed of the internal combustion engine and compressor may change at any time during working hours. For fixed-pad rotating machinery, it is not suitable for these time-varying working states, nor can it adjust its working parameters according to actual working requirements. This may cause safety problems such as excessive rotor vibration or oil film instability and seriously affects the stable operation of rotor bearing system. Therefore, in order to improve the stability of the rotor system, it is necessary to propose a reasonable adjustable bearing structure and adjustment method.

The dynamic characteristics of the rotor bearing system under variable operating conditions have been the focus of scholars. In order to make the rotating machine safe and stable, many methods for suppressing the vibration of the rotor have been proposed. Combining the demand for optimum operation, suppressed vibration amplitude and enhanced stability, the concept of adjustable/controllable journal bearing has been developing in the last six to seven decades. Rao and Tiwari [1, 2] have proposed single objective and multi-objective genetic algorithms for active control system of active magnetic bearing (AMB) and optimized the design method of active thrust hybrid magnetic bearing. Dohnal and Markert [3] achieves periodic open-loop control of the stiffness coefficient of a bearing by periodically changing the control parameters of an active magnetic bearing. This periodic variation can enhance the effective damping of the rotor system, resulting in reduced vibration. Palazzolo and Lin [4] studied the application of piezoelectric actuators in active vibration control of rotating machinery. The test results show significant reduction in unbalance, transient, and subsynchronous responses.

Tuma et al. [5] proposes a working prototype of a system for the active vibration control of journal bearings with the use of piezoactuators. The results show that the active vibration control considerably extends the range of the operational speed. Ishida and Liu [6] proposed a discontinuous spring concept that uses discrete spring characteristics to suppress rotating mechanical vibrations. Santos and Nicolettid [7–10] through the hydraulic control system, change the journal bearing lubrication performance, found the feasibility of attenuating rotor vibrations in test rigs with rigid rotors. Krodkiewski et al. [11–13] studied the active journal bearing with a flexible sleeve. The damper selects the optimal damping coefficient to significantly improve the stability of the system's equilibrium position. Chasalevris and Dohnal [14–17] proposed a journal bearing with an variable geometry and found that the bearing can effectively reduce the maximum amplitude of the journal passing through the critical speed. When the bearing is applied to a large rotor-bearing system, the operating stability of the rotor system can be effectively improved. Sivrioglu [18] proposed an adaptive control method and calculates the nonlinear control current of the zero bias magnetic bearing to improve the adaptability of the control system to the dynamic behavior of the spindle. Iwada and Nonami [19] use the self-optimization theory of bearing support to study rotor vibration control based on self-optimizing support system. Reinig and Desrochers [20] utilize the disturbance regulation controller of the rotating mechanical system to suppress the vibration of the rotating machinery. In addition, some scholars have combined the advantages of journal bearings and AMBs to control the instability of journal bearings using the control method of AMBs [18–20]. At present, academic circles have put forward many methods for improving the stability of the rotor-bearing system, and have also

achieved many academic achievements in the theoretical and experimental research process. However, only some methods would meet a practical application of industrial rotating machinery due to cost, simplicity, and reliability.

This study proposes a new type of adjustable bearing structure that achieves the function of changing the characteristic parameters of the bearing under continuous operating conditions. The adjustable bearing is based on the principle of mechanical transmission and applies active control to the fluid bearing. The device can change the stiffness and damping of the oil film according to the actual vibration of the rotor. Compared with the traditional fixed-pad bearing, the adjustable bearing is more suitable for changing working conditions. By formulating a reasonable control strategy to select a reasonable oil film thickness for different working conditions, the stability and reliability of the rotating machine can be significantly improved. This paper first studies the working principle of the adjustable bearing and calculated the displacement of the bearing pads resulting in the change of stiffness and damping matrix. With these results, the next step is to thoroughly study the effect of adjustable bearings on the stability of the rotor system.

## 2 Design and operation principle of adjustable bearing

The adjustable bearing consists of upper and lower pads (Fig. 1). The upper bearing pad is fixed, and the lower pad slides up and down along the guide rail in a vertical direction under the action of the inclined iron. When the lower pad moves upward, the oil film clearance of the bearing decreases. The thinner the oil film, the larger the pressure gradient, which causes the oil film to withstand greater journal pressure. However, when the pressure provided by the oil film is greater than the load on the journal, half-frequency whirl and oil film oscillation are likely to occur. When the lower pad moves downward, the oil film clearance of the bearing increases. The thicker the oil film, the smaller the pressure gradient, which causes the bearing capacity of the oil film to decrease. This may cause vibration and wear failure of the rotating machine. However, the downward movement of the lower pad reduces the working position of the journal, which can effectively eliminate oil film instability and improve system stability. Therefore, in the operation of the rotating machinery, the selection of a reasonable oil film thickness has a significant impact on the stability of the rotor system.

The structural design of the adjustable bearing and the definition of each component are shown in Fig. 2. The working principle of the adjustable bearing is that the rotation of the lead screw drives the horizontal movement of the inclined iron. The inclined iron pushes the bearing lower pad to slide up and down along the guide rail, thereby causing the oil film clearance of the bearing to change. When the vibration of the journal does not meet the requirements of the working condition, the thickness of the oil film is changed by adjusting the lead screw to improve the stability of the rotor system. The bearing structure is based on the mechanical transmission principle, and the active control is applied to the fluid bearing. The bearing ellipticity can be adjusted according to the actual vibration condition of the rotor at different speeds. The vibration of the rotor can be suppressed by changing the thickness of the oil film so that the vibration amplitude

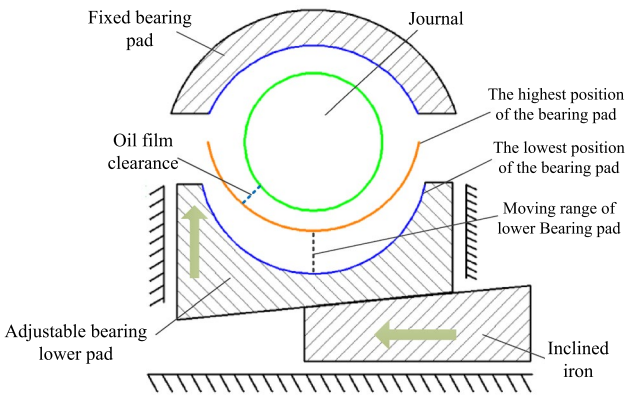


**Fig. 1** Schematic diagram of the adjustable bearing structure and the movable position of the bearing pad

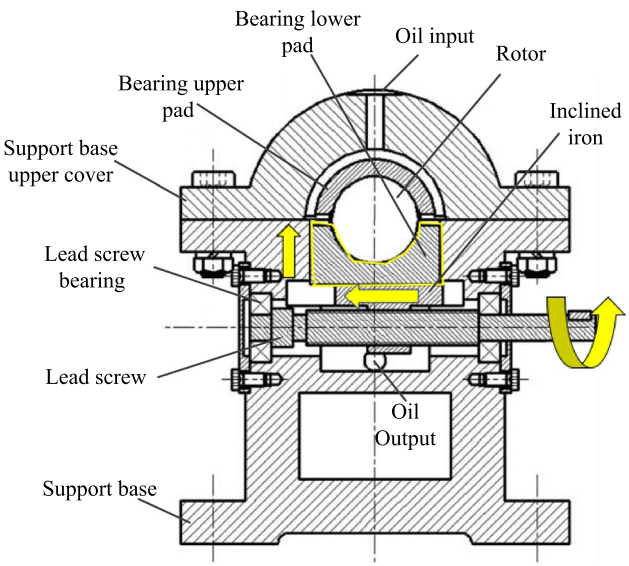


**Fig. 2** Structural design of adjustable bearing and definition of components

during the acceleration of the rotor is always within the safe range.

Adjusting the bearing oil film clearance through a mechanical transmission system is an important feature of an adjustable bearing. The mechanical transmission system has high reliability and a large bearing capacity. When the mechanical transmission system is applied to the journal bearing, it improves the working state of the journal bearing under different working conditions.

## 3 Evaluation of the adjustable bearing dynamic characteristics

The adjustable bearing has the ability to adjust the thickness of the oil film, and the different thickness of the oil film results in different dynamic characteristics of the rotor system. The influence of the adjustable bearing on the dynamic characteristics of the bearing is studied below. With these results, the influence of adjustable bearing on rotor system stability can be thoroughly studied next.

$$e_1 = \sqrt{e^2 + (e')^2 + 2ee'\cos\theta} \qquad e_2 = \sqrt{e^2 + (e')^2 - 2ee'\cos\theta} \tag{1}$$

$$\theta_1 = \arcsin\frac{e\sin\theta}{e_1}$$
$$\theta_2 = \arcsin\frac{e\sin\theta}{e_2} \tag{2}$$

The positional relationship between the journal and the bearing pad under the working condition of the adjustable bearing is shown in Fig. 3. The following formulas define the bearing operational parameters in correspondence to Fig. 3. The center of the journal is ***O'*** and the preset eccentricity of the bearing is ***e'***. When the working state of the journal changes, the adjustable bearing can adjust the preset eccentricity ***e'*** to improve the dynamic characteristics of the rotor bearing system. The positional relationship between the upper and lower pads and the journal can be calculated according to the geometric relationship shown in the figure, such as Eq. (1) and Eq. (2).

Under working conditions, the upper and lower pads of the adjustable bearing both are the oil film pressure bearing zone. According to the positional relationship between the journal and the bearing pad, the oil film thickness expression of the upper and lower tiles is calculated as Eq. (3).

$$h = \begin{cases} C + \sqrt{e^2 + (e')^2 + 2ee'\cos\theta}\cos(\phi - \theta_1) \\ C + \sqrt{e^2 + (e')^2 - 2ee'\cos\theta}\cos(\phi - \pi + \theta_2) \end{cases} \tag{3}$$

When the center ***O'*** of the journal coincides with the geometric center ***O*** of the bearing (Fig. 4), the

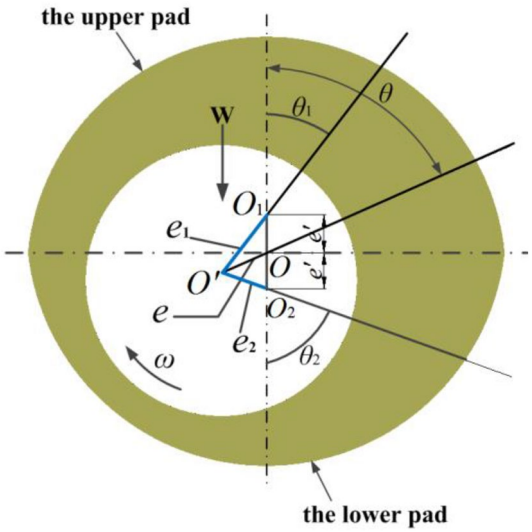


**Fig. 3** Schematic diagram of the positional relationship between the journal and the bearing bush under the working condition of the adjustable bearing

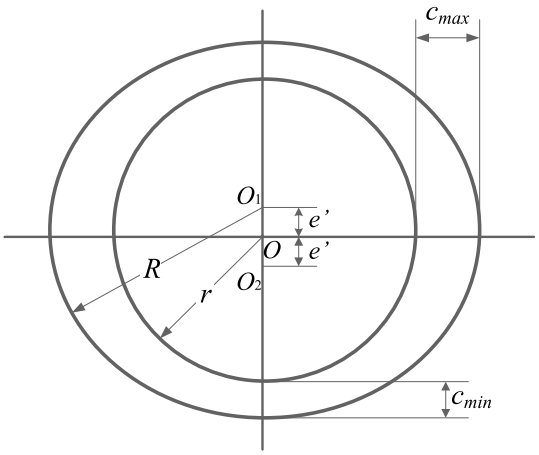


**Fig. 4** Geometric relationship between preset Eccentricity, top clearance and side clearance of elliptical bearing

maximum value of the adjustable bearing radius clearance is $c_{max} \approx c_r (c_r = R - r)$, and the minimum value is $c_{min} = c_r - e'$.

Ellipticity of an adjustable bearing is defined as:

$$\delta = \frac{e'}{c_r} = 1 - \frac{c_{min}}{c_{max}}.$$

The ellipticity is an important bearing parameter for adjustable bearings. In this study, the adjustment of the ellipticity has a crucial influence on the stability of the rotor system. Reasonably adjusting the ellipticity can greatly improve the stability of the rotor system. In order

to make the adjustable elliptical bearing to have a significant effect of suppressing vibration, the oil film clearance of the adjustable elliptical bearing is designed to have a larger adjustment range. The ellipticity in this study varies from 0 to 0.7. In the following theoretical and experimental studies, the ellipticity is used an the adjustment parameter. By studying the dynamic characteristics of the rotor system at different ellipticity, the method of improving the stability of a rotor system by an adjustable bearing is obtained.

In order to find out a reasonable regulation scheme to improve the stability of the rotor system, it is necessary to study the dynamic characteristics of the bearing under different ellipticity. The dynamic characteristics of the adjustable bearing are calculated and evaluated below. Adjustable bearing upper and lower pads are oil film pressure bearing areas, so the dynamic characteristics of the two bearing pads need to be calculated separately.

When calculating the oil film stiffness and damping coefficient, it is necessary to first solve the equilibrium position ($\theta$, e) of the journal in the bearing, and then calculate the eccentricity and the attitude angle of the upper and lower pads according to Eq. (1) to (2). The eccentricity and the attitude angle of the upper and lower pads are brought into Eq. (3) to calculate the oil film thickness of the upper and lower pads. The calculated thickness of the oil film is brought into the Reynolds equation in Eq. 4, and then, the differential equations of disturbance pressures are obtained by solving the partial derivative of Reynolds equation, in Eq. (5). Finally, the dynamic coefficients of the oil film are obtained by integrating the differential equations, in Eq. (6).

The angle $\varphi_{11}$ is the angle of the beginning of the lower pad oil film while $\varphi_{12}$ is the angle of the end of the lower pad oil film. The angle $\varphi_{21}$ is the angle of the beginning of the upper pad oil film while $\varphi_{22}$ is the angle of the end of the upper pad oil film. The formula for the damping coefficient is basically the same as the formula for calculating the stiffness coefficient, which is not included in this paper.

$$\frac{\partial}{\partial\varphi}\left(h^3\frac{\partial P}{\partial\varphi}\right)+\left(\frac{d}{l}\right)^2\frac{\partial}{\partial\lambda}\left(h^3\frac{\partial P}{\partial\lambda}\right)=3\frac{\partial h}{\partial\varphi}+6\left(\varepsilon cos\varphi+\varepsilon\theta' sin\varphi\right) \tag{4}$$

$$\begin{aligned}
K_{xx}&=-\int_0^1\int_{\varphi_{11}}^{\varphi_{12}}P_e\cos\left(\theta_1+\varphi_1\right)d\varphi_1 d\lambda-\int_0^1\int_{\varphi_{21}}^{\varphi_{22}}P_e\cos\left(\varphi_2-\theta_2\right)d\varphi_2 d\lambda\\
K_{xy}&=-\int_0^1\int_{\varphi_{11}}^{\varphi_{12}}P_e\sin\left(\theta_1+\varphi_1\right)d\varphi_1 d\lambda-\int_0^1\int_{\varphi_{21}}^{\varphi_{22}}P_e\sin\left(\varphi_2-\theta_2\right)d\varphi_2 d\lambda\\
K_{yx}&=-\int_0^1\int_{\varphi_{11}}^{\varphi_{12}}P_\theta\cos\left(\theta_1+\varphi_1\right)d\varphi_1 d\lambda-\int_0^1\int_{\varphi_{21}}^{\varphi_{22}}P_\theta\cos\left(\varphi_2-\theta_2\right)d\varphi_2 d\lambda\\
K_{yy}&=-\int_0^1\int_{\varphi_{11}}^{\varphi_{12}}P_\theta\sin\left(\theta_1+\varphi_1\right)d\varphi_1 d\lambda-\int_0^1\int_{\varphi_{21}}^{\varphi_{22}}P_\theta\sin\left(\varphi_2-\theta_2\right)d\varphi_2 d\lambda
\end{aligned} \tag{6}$$

The above description briefly introduces the calculation process of the dynamic coefficient of the adjustable bearing. The dynamic coefficient of the adjustable bearing can be calculated by using Eq. (6). In order to study the influence of ellipticity on the stability of the rotor system, the above formula is used to calculate the change of stiffness and damping coefficient during the acceleration process of the rotor system under different ellipticities, Fig. 5. The calculations find that as the rotational speed increases, the rotor center position moves up, and the stiffness and damping coefficient of the oil film in both the vertical and horizontal directions decrease. At the same speed, the greater the ellipticity, the greater the stiffness and damping coefficient. As such, adjusting the ellipticity can change the dynamic characteristics of the bearing.

The effect of ellipticity on the trend of stiffness and damping coefficient at a fixed speed (see Fig. 6). From the calculation, as the ellipticity increases, the stiffness and damping coefficient in the vertical direction change significantly, and the stiffness and damping coefficient in the horizontal direction change less. This is because when the ellipticity increases, the bearing lower pad moves upward, the top clearance decreases, and the side clearance remains unchanged. In this way, the stiffness and damping coefficient of the vertical direction will change greatly, while the horizontal stiffness and damping coefficient will remain unchanged. When the

$$\begin{aligned}
&\frac{\partial}{\partial\varphi}\left(h^3\frac{\partial P_e}{\partial\varphi}\right)+\left(\frac{d}{l}\right)^2\frac{\partial}{\partial\lambda}\left(h^3\frac{\partial P_e}{\partial\lambda}\right)=-3\sin\varphi-\frac{9}{h}cos\varphi\frac{\partial h}{\partial\varphi}+3h\left[\left(cos\varphi\frac{\partial h}{\partial\varphi}+sin\varphi h\right)\frac{\partial P}{\partial\varphi}+\left(\frac{d}{l}\right)^2cos\varphi\frac{\partial h}{\partial\lambda}\frac{\partial P}{\partial\lambda}\right]\\
&\frac{\partial}{\partial\varphi}\left(h^3\frac{\partial P_\theta}{\partial\varphi}\right)+\left(\frac{d}{l}\right)^2\frac{\partial}{\partial\lambda}\left(h^3\frac{\partial P_\theta}{\partial\lambda}\right)=3cos\varphi-\frac{9}{h}\sin\varphi\frac{\partial h}{\partial\varphi}+3h\left[\left(\sin\varphi\frac{\partial h}{\partial\varphi}+cos\varphi h\right)\frac{\partial P}{\partial\varphi}+\left(\frac{d}{l}\right)^2\sin\varphi\frac{\partial h}{\partial\lambda}\frac{\partial P}{\partial\lambda}\right]\\
&\frac{\partial}{\partial\varphi}\left(h^3\frac{\partial P_{\dot e}}{\partial\varphi}\right)+\left(\frac{d}{l}\right)^2\frac{\partial}{\partial\lambda}\left(h^3\frac{\partial P_{\dot e}}{\partial\lambda}\right)=6cos\varphi\\
&\frac{\partial}{\partial\varphi}\left(h^3\frac{\partial P_{\dot\theta}}{\partial\varphi}\right)+\left(\frac{d}{l}\right)^2\frac{\partial}{\partial\lambda}\left(h^3\frac{\partial P_{\dot\theta}}{\partial\lambda}\right)=6\sin\varphi
\end{aligned} \tag{5}$$

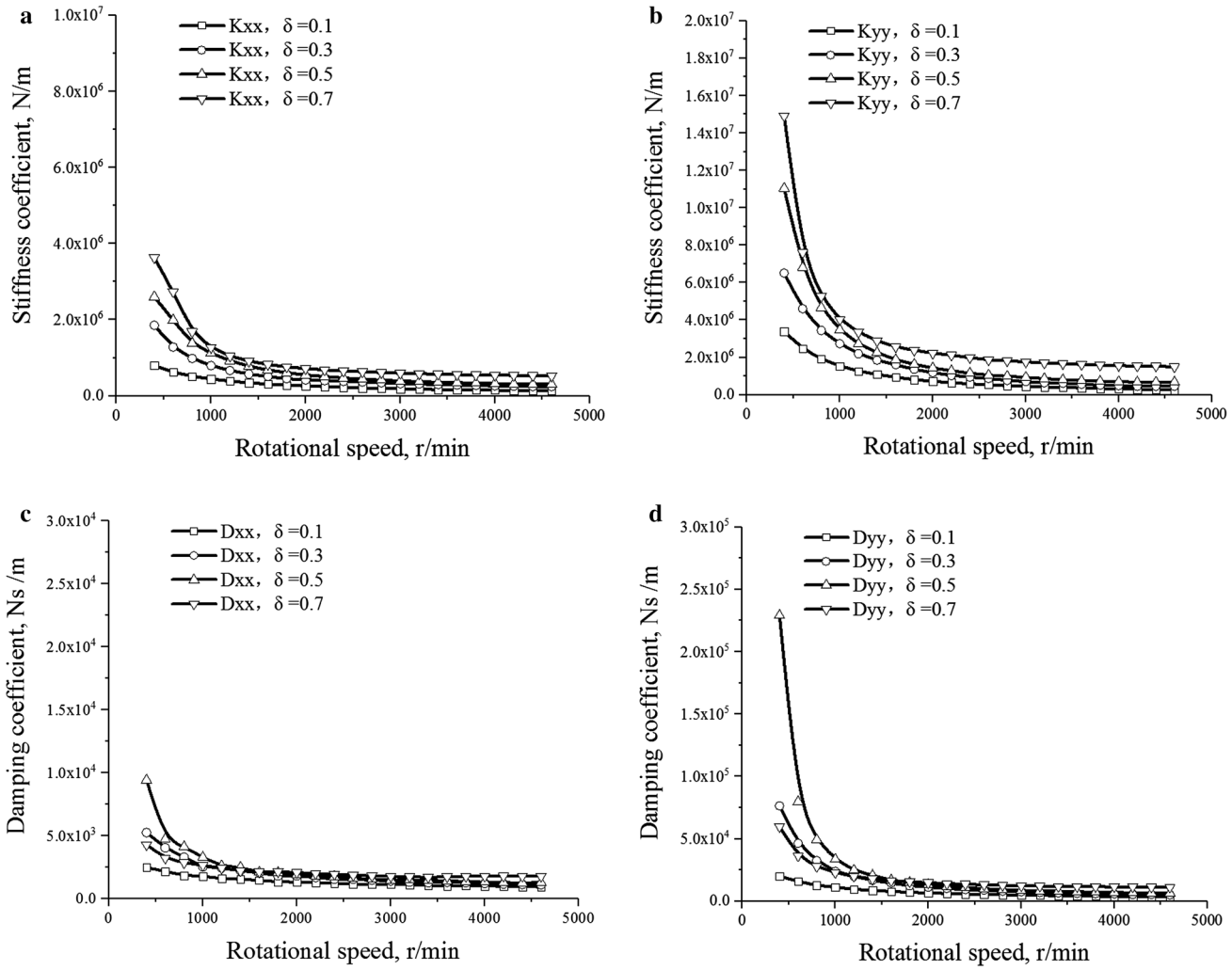


**Fig. 5** Stiffness and damping coefficients of the adjustable bearing as a function of rotational speed, **a** is the horizontal stiffness, **b** is the vertical stiffness, **c** is the horizontal damping, **d** is the vertical damping

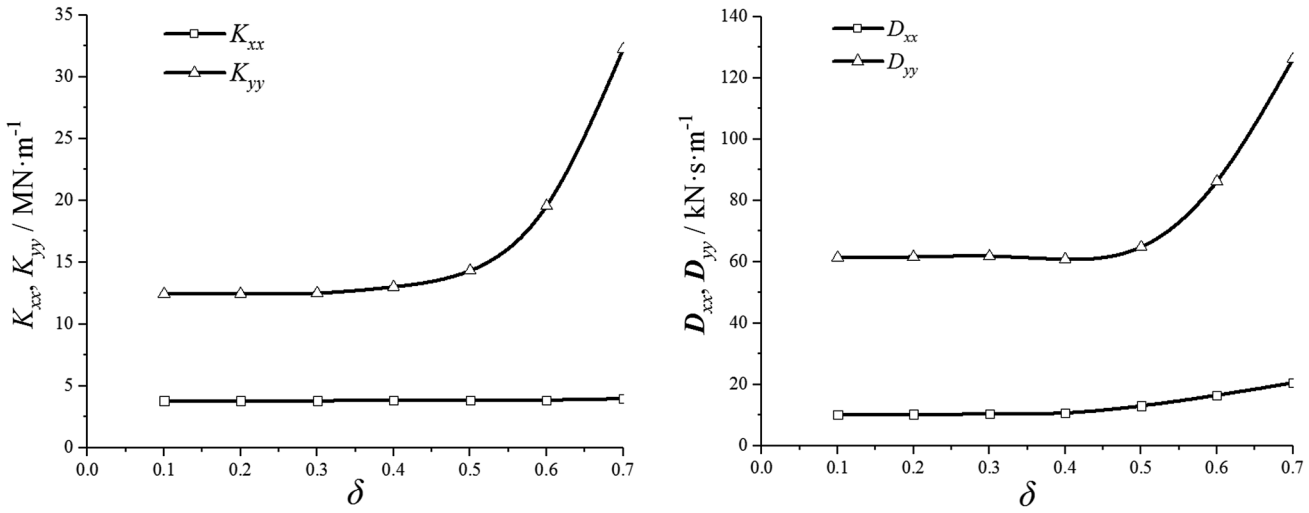


**Fig. 6** Stiffness (left) and damping (right) coefficients of the adjustable bearing as a function of ellipticity

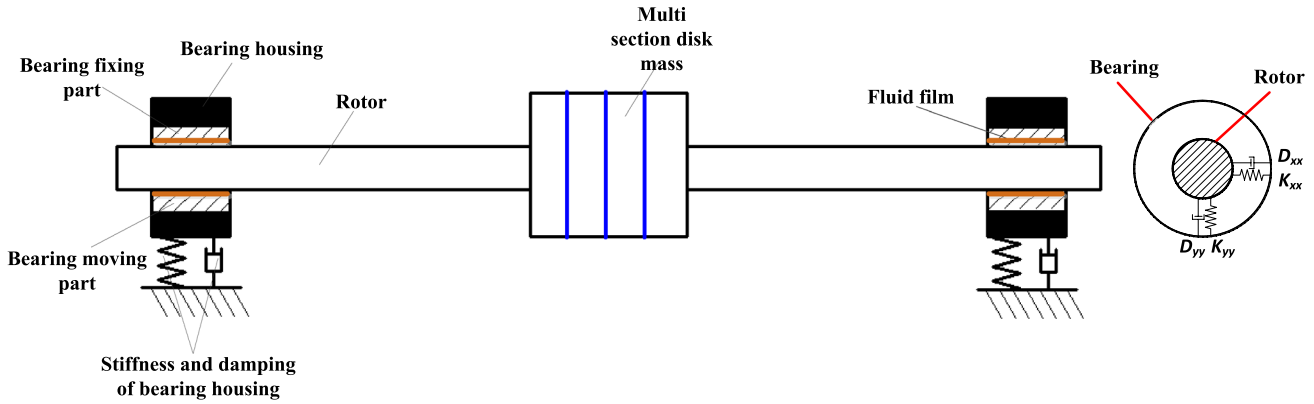


**Fig. 7** Representation of an adjustable bearing rotor system

**Table 1** Physical and geometrical properties of the rotor bearing system

| | | | |
|---|---|---|---|
| Young's modulus: | E = 206 GPa | Disc width | $L_d$ = 0.090 m |
| Material density | $\rho$ = 7850 kg/m$^3$ | Disc mass | $m_d$ = 29.3 kg |
| Lubricant viscosity | $\mu$ = 0.011 Pa s | Shaft mass | $m_s$ = 13.2 kg |
| Bearing radius | $R_b$ = 0.020 m | Bearing radial clearance | $c_r$ = 0.0002 m |
| Shaft radius | $R_s$ = 0.020 m | Ellipticity | $\delta$ = 0–0.7 |
| Disc radius | $R_d$ = 0.120 m | Shaft span | $L$ = 1.2 m |

ellipticity increases from 0.1 to 0.7, the vertical stiffness increases to 2.5 times the initial value, the horizontal stiffness increases by 0.3 times, the vertical damping increases to 2 times the initial value, and the horizontal damping increases by 0.7 times. The variation law of the adjustable bearing stiffness and damping under different ellipticity can provide reference for the following dynamics research.

## 4 Theoretical application of the adjustable journal bearing in a rotor-bearing system

The dynamic characteristics of the rotor system during the acceleration process of the rotating machine will change greatly. When approaching the critical speed (resonant frequency), the amplitude of the rotor will increase sharply. Excessive vibration will threaten the safe operation of the rotor system. The following applies the adjustable bearing to the rotating machine to simulate the effect of the adjustable bearing on the stability of the rotating machine. In order to study the effect of ellipticity on the stability of the rotor system, a simple flexible rotor model is established, as shown in Fig. 7. The rotor bearing system model parameters are shown in Table 1.

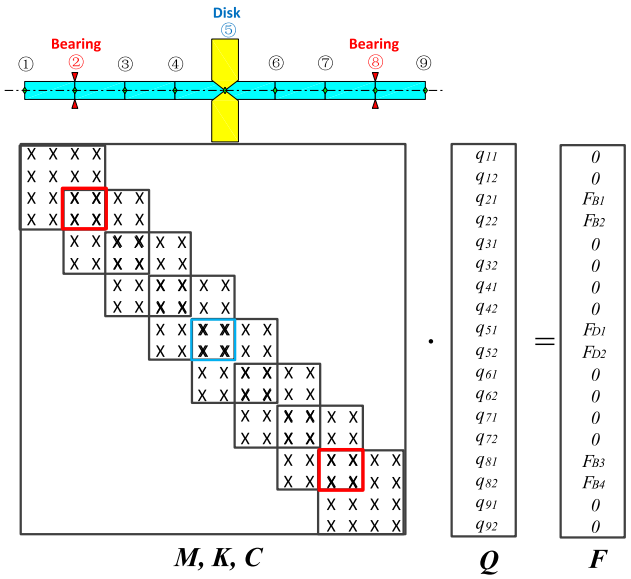


**Fig. 8** The assembly of the finite element model of the rotor-bearing system, which defines the matrices ***P***, ***Q*** and ***F*** according to the geometry of the rotor-bearing system

According to the structural parameters of the rotor system (Table 1), the corresponding rotor bearing system finite element model is established. The whole finite element model is separated into nine nodes, a total of eight elements (Fig. 8). Among them, ***P (M K C)*** represents the mass matrix, stiffness matrix and damping matrix of rotor system, ***Q*** represents the degree of freedom of the system, and ***F*** represents the load of the system. The bearing matrix is distributed at second and eighth nodes, and the mass disk matrix is located at fifth nodes. When the ellipticity of the system changes, we only need to introduce the stiffness and damping of the corresponding ellipticity into the matrix of the bearing node, and then establish the corresponding dynamic equation to solve the response.

The dynamic equation of the rotor bearing system is defined as Eq. 7.

$$M\ddot{q}(t) + C\dot{q}(t) + Kq(t) = F(t) \tag{7}$$

The vibration response calculation formula is defined as Eq. 8.

$$q = [-\Omega^2 M + \mathrm{j}\Omega(\Omega G + C) + K]^{-1} \cdot \Omega^2 \begin{Bmatrix} m\varepsilon e^{\mathrm{j}\delta} \\ -\mathrm{j}m\varepsilon e^{\mathrm{j}\delta} \\ \mathrm{j}(I_d - I_p)\beta e^{\mathrm{j}\gamma} \\ (I_d - I_p)\beta e^{\mathrm{j}\gamma} \end{Bmatrix} \tag{8}$$

where ***M*** is the structural mass matrix; ***C*** is the damping matrix; ***K*** is the structural stiffness matrix; ***q*** is the displacement matrix; ***F*** is the load matrix. The damping matrix ***C*** takes into account the gyro effect and the Rayleigh damping matrix. The Rayleigh damping matrix is a linear combination of ***M*** and ***K***, that is $\alpha M + \beta K$, where $\alpha$ and $\beta$ are constants independent of frequency, which are related to the damping coefficient and the previous two natural frequencies of the system. ***F*** consists of unbalanced forces and gravity. ***G*** is the gyro matrix. m is the total mass of the rotor, $\varepsilon$ is the eccentricity, $\Omega$ is the angular velocity of the rotor, $\delta$ is the phase angle, $I_d$ is the moment of inertia of the rotor, and $I_p$ is the polar moment of inertia of the rotor, $\gamma = I_p / I_d$.

The dynamic response of the rotor system with different ellipticity is studied by using the rotor-bearing system model shown in Fig. 7. According to the variation of the stiffness and damping of the bearing under the different ellipticity in Fig. 6, the stiffness and damping values are respectively introduced into the dynamic equations. The dynamic equation is solved by Runge–Kutta variable step integral and get the dynamic response of the rotor acceleration process.

The vibration response of the rotor during the acceleration process at different ellipticities is shown in Figs. 9 and 10. The rotor is accelerated at a constant acceleration of 1.5 rad/s$^2$. The ellipticity of the first acceleration process is 0.2, the second acceleration process is 0.7, and the other operating conditions are identical.

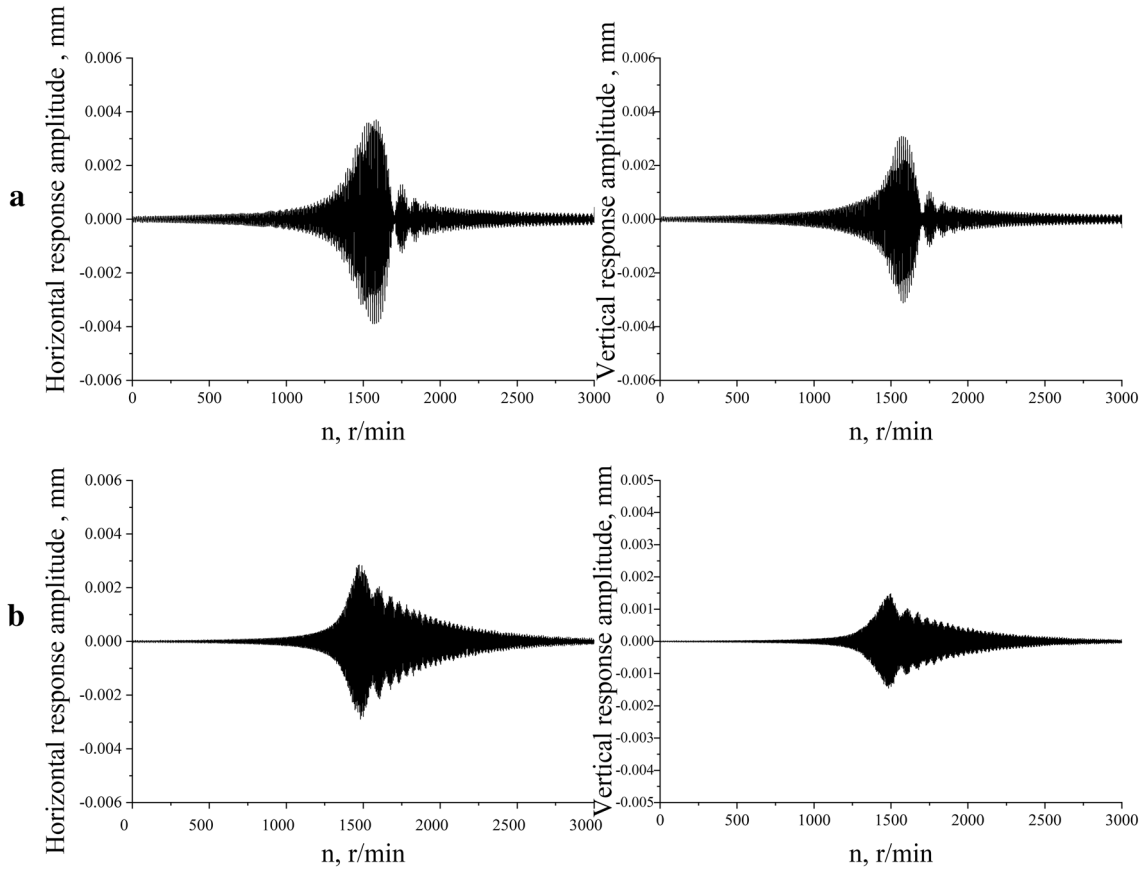


**Fig. 9** Amplitude of the response of the journal during acceleration process under different ellipticity, **a** is the first acceleration process, **b** is the second acceleration process)

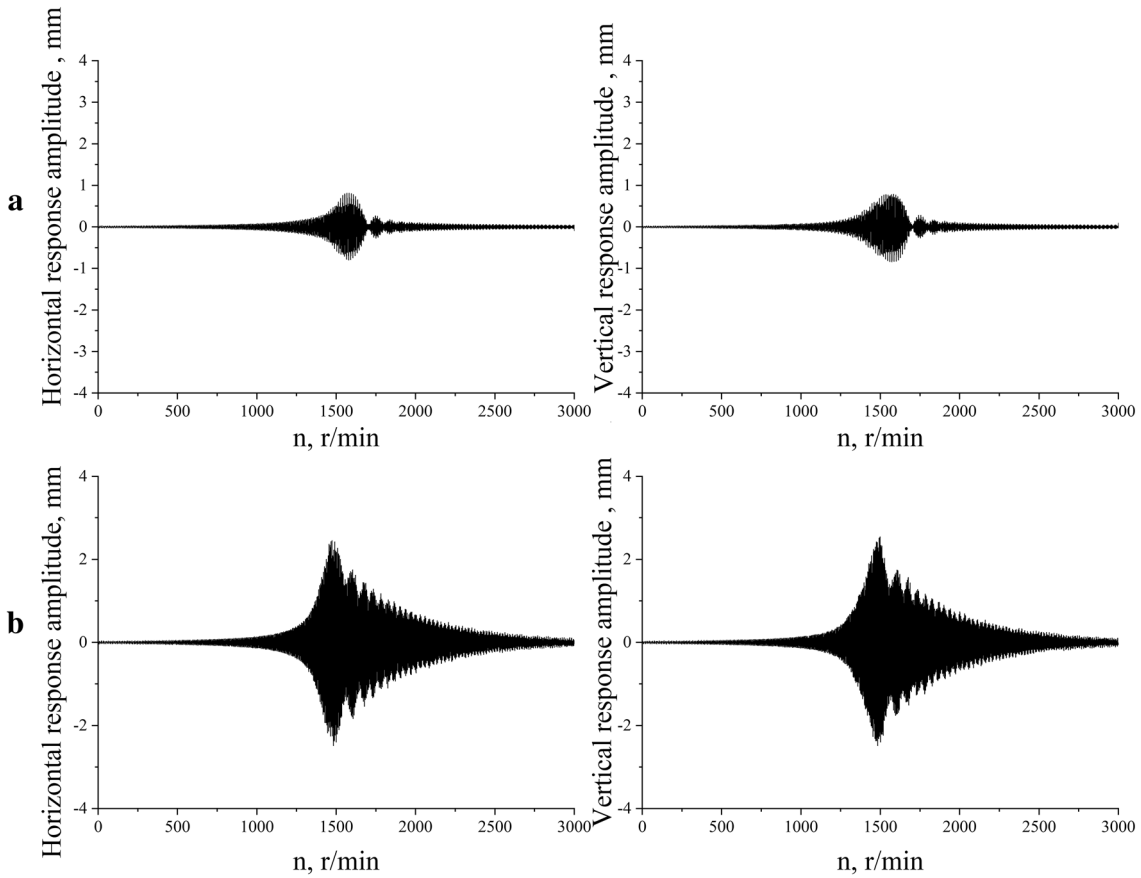


**Fig. 10** Amplitude of the response of the rotor disk during acceleration process under different ellipticity, **a** is the first acceleration process, **b** is the second acceleration process

The variation of the journal amplitude of the bearing position under different ellipticity is shown in Fig. 9. When the critical speed is approached, the amplitude of the journal changes relatively greatly. The first acceleration has an ellipticity of 0.2, the maximum amplitude of the bearing position in the horizontal direction is 0.004 mm, and the maximum amplitude in the vertical direction is 0.0037 mm. The second acceleration process has an ellipticity of 0.7, a maximum amplitude of the bearing position in the horizontal direction of 0.0027 mm, and a maximum amplitude in the vertical direction of 0.0015 mm. The calculations find that by increasing the ellipticity, the amplitude of the bearing position journal can be effectively reduced. The amplitude is decreased by the same extent in both the vertical and horizontal directions.

The amplitude variation of the rotor at the mass disk position under different ellipticities is shown in Fig. 10. The ellipticity of the first acceleration process is 0.2, the maximum amplitude of the rotor in the horizontal direction of the mass disk position is 0.95 mm, and the maximum amplitude in the vertical direction is 0.92 mm. The ellipticity of the second acceleration process is 0.7, the maximum amplitude of the rotor in the horizontal direction is 2.44 mm, and the maximum amplitude in the vertical direction is 2.45 mm. The calculations find that the amplitude of the mass disk near the critical speed increases obviously with increasing ellipticity. During the two accelerations, the change trend of the mass disk position is completely opposite to the change trend of the bearing position. It is necessary to further analyze the cause of this phenomenon and determine a reasonable ellipticity adjustment mode.

During the first acceleration, the amplitude of the rotor quickly decreases after the speed exceeds the critical speed, and returns to a stable operation state, as shown in Figs. 9a and 10a. During the second acceleration process, the amplitude of the rotor continues to be in a dangerous state after the speed exceeds the critical speed, and it takes a longer time to return to the stable operation state, as shown in Figs. 9b and 10b. In response to this phenomenon, vibration data at a rotational speed of 1800 rpm (critical speed of 1500 rpm) was extracted,

and the vibration of the rotor was analyzed. The data with the speed of 1800 rpm is selected for analysis to determine whether the oil film whirl occurs after the rotor crosses the critical speed.

The vibration data at a rotational speed of 1800 rpm was extracted, and data analysis was performed by plotting the axis orbit and the vibration frequency amplitude. The analysis result of the vibration data of the rotor is shown in Fig. 11. The first acceleration process has an ellipticity of 0.2, the rotor's axis orbit is small, and the vibration frequency is only the Co-frequency vibration, indicating that the rotor system is running very stable. When the ellipticity of the second acceleration process is adjusted to 0.7, the axis orbit of the rotor increases obviously, and there are two vibration frequency components, the Co-frequency vibration and half-frequency whirling. The occurrence of half-frequency whirling vibration frequency indicates oil film whirl in the rotor system, and the rotor system has safety hazards.

The analysis result of the vibration data of the journal is shown in Fig. 12. The ellipticity is adjusted from 0.2 to 0.7, the axis orbit of the journal is significantly reduced, and the vibration amplitude of the co-frequency vibration frequency is also significantly reduced. However, the half-frequency whirl frequency appears. This indicates that although the vibration amplitude of the rotor is reduced, there is hidden danger.

The analysis results show that it is not feasible to reduce the amplitude of the critical speed of the rotor by increasing the ellipticity, which may lead to oil film instability.

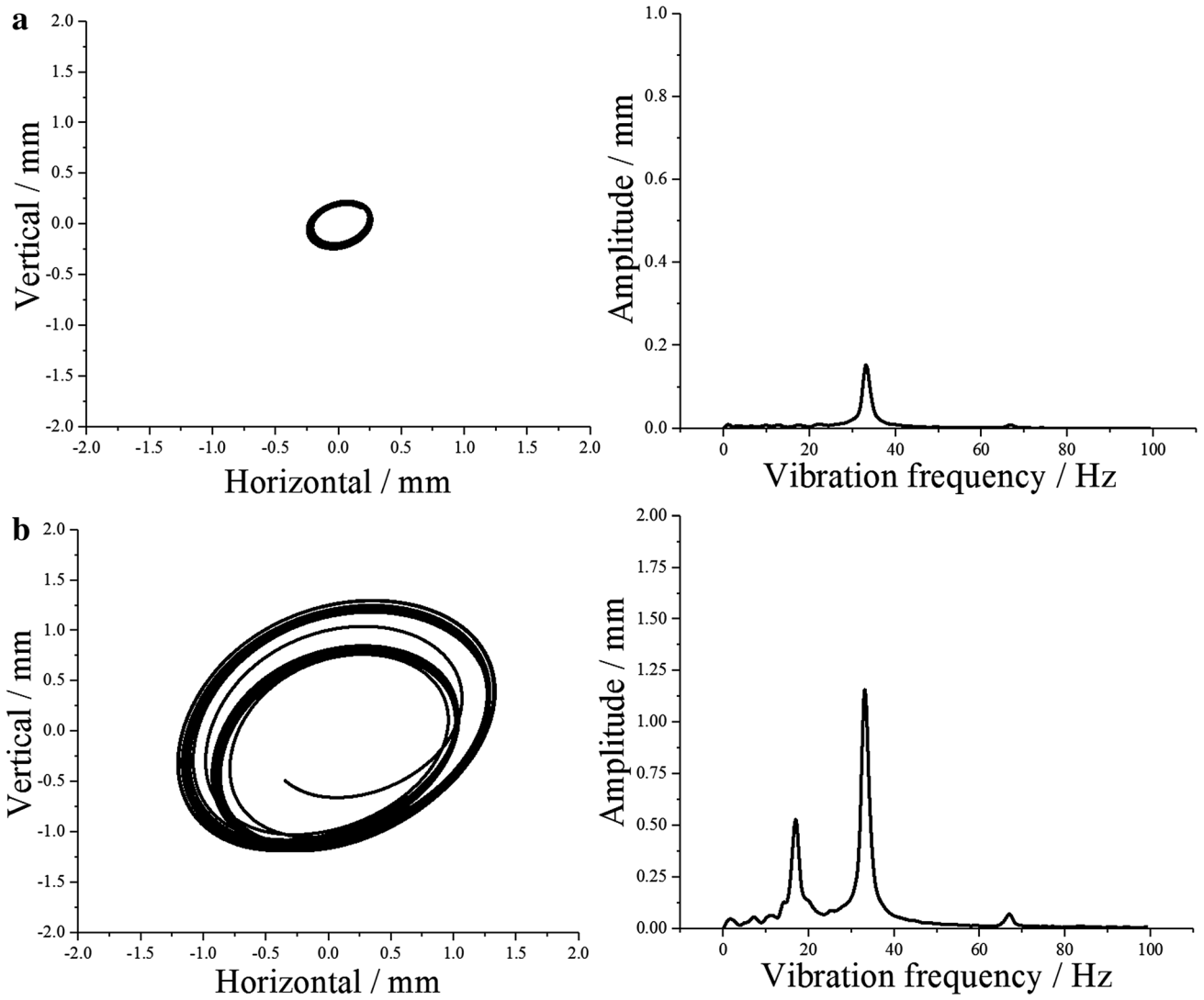


**Fig. 11** Axis orbit and vibration frequency amplitude of the rotor at the mass disk position at 1800 rpm, **a** is the first acceleration process, **b** is the second acceleration process

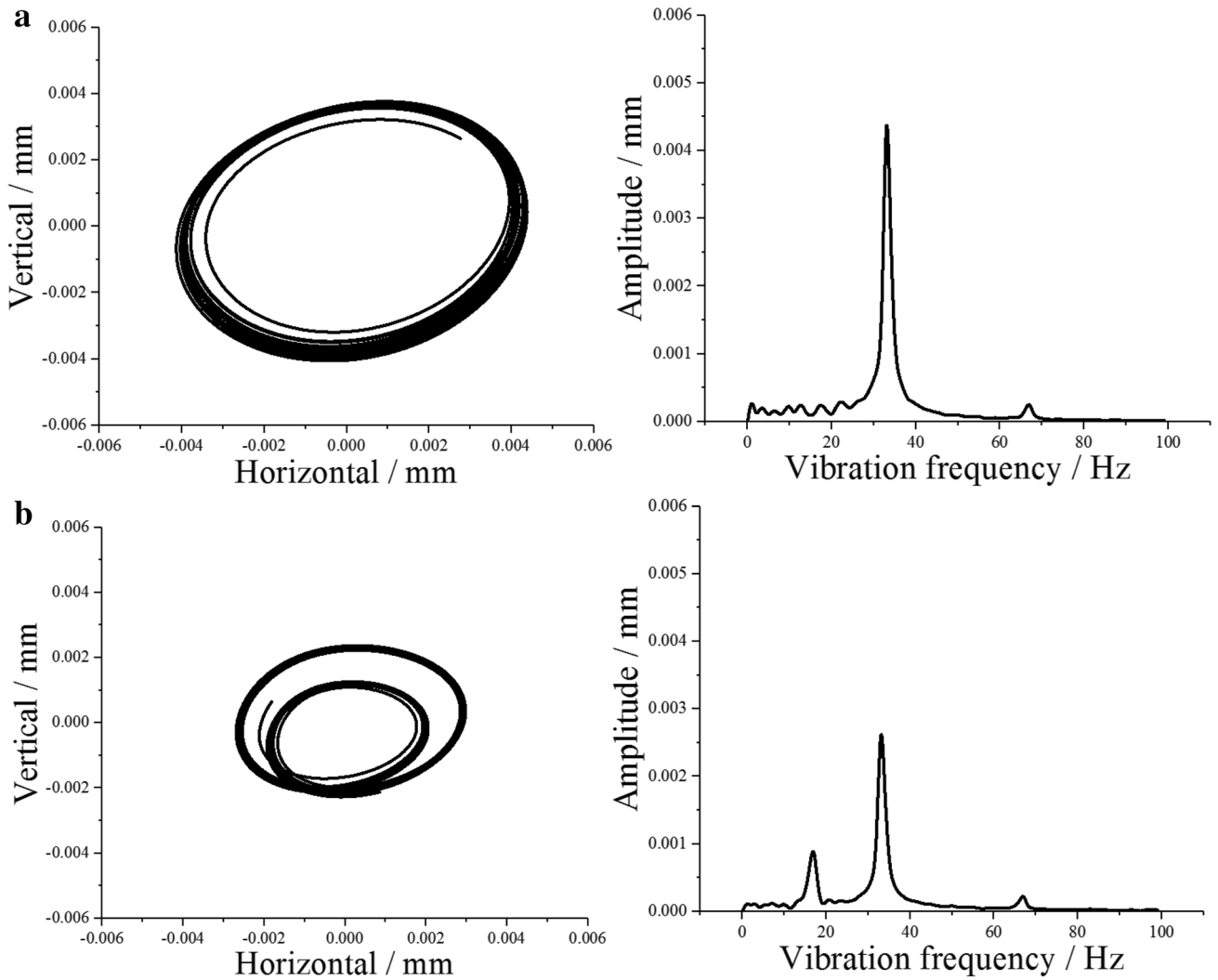


**Fig. 12** Axis orbit and vibration frequency amplitude of the journal at 1800 rpm, **a** is the first acceleration process, **b** is the second acceleration process)

The correct adjustment method is to reduce the ellipticity when the critical speed is exceeded, and to improve the stability of the rotor system by increasing the oil film clearance.

## 5 Experimental application of adjustable bearing in rotor acceleration process

In order to study the influence of adjustable bearings on the stability of the rotor system, a rotor bearing test rig was designed and built. The experimental test rig layout and data acquisition scheme are shown in Fig. 13. The main physical and geometrical properties of the experimental test rig are listed in Table 1. The adjustable bearing is installed in the bearing housing at the right end of the test bench. During the test, the bearing ellipticity can be adjusted according to the working conditions. This test simulates the acceleration process of the rotor system, the speed is uniformly accelerated from 0 to 3000 rpm in 20 s, and then rotated at a fixed speed of 3000 rpm. Among them, 1500 rpm is the first critical speed of the rotor system

During the start-up of the rotor system, the working position of the rotor floats as the rotational speed increases. The rotor speed reaches twice the critical speed, and oil film instability may occur under light load conditions or sudden load reduction. In the following experiment, no load was applied to the rotor system and it was uniformly accelerated to 3000 rpm, which caused oil film whip in the rotor system (see Fig. 14). Adjusting the ellipticity under this condition to study the effect of adjustable bearings on the stability of the rotor system.

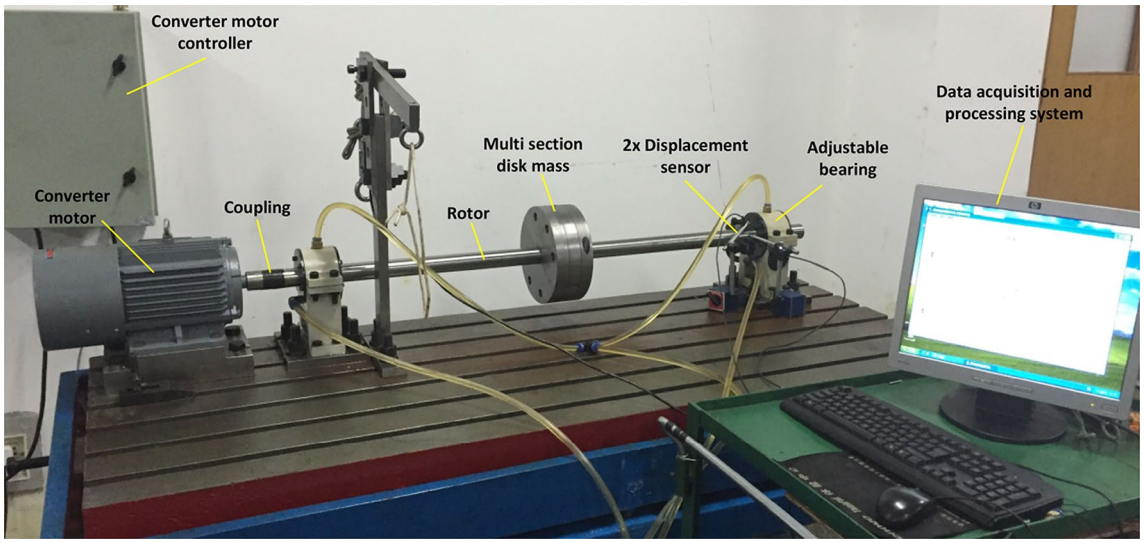


**Fig. 13** View and description of the experimental test rig layout

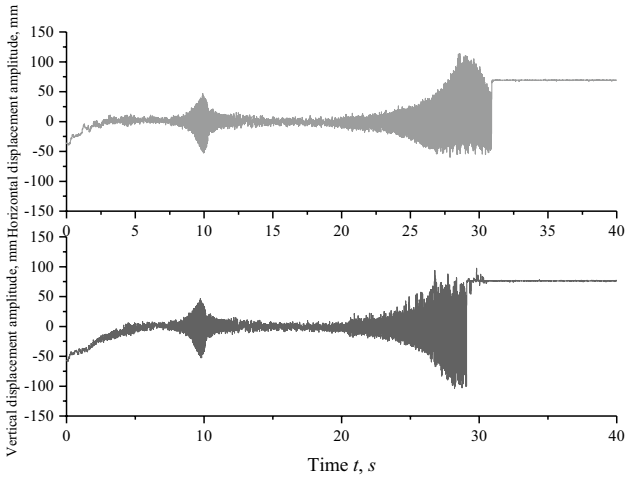


**Fig. 14** Journal displacement at the locations of the adjustable bearings as a function of time. In the first experimental procedure, the ellipticity was not adjusted, the oil whip occurred in the 20th second, and the rotor system was forced to close at the 30th second

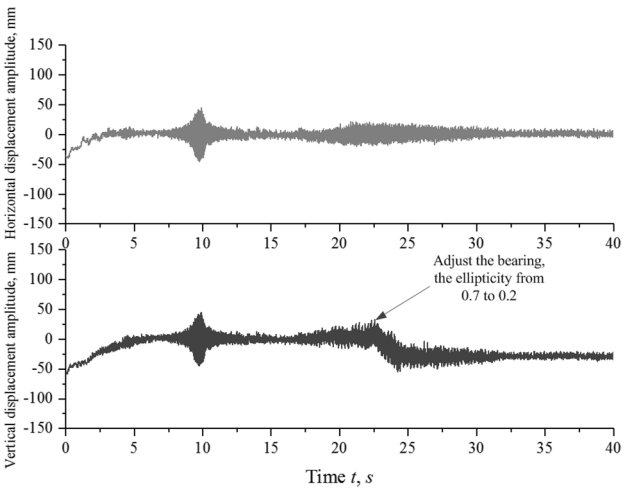


**Fig. 15** Journal displacement at the locations of the adjustable bearings as a function of time. In the second experimental procedure, the ellipticity was adjusted from 0.7 to 0.2 at the 23rd second

The first acceleration process is shown in Fig. 14. The rotor system successfully crossed the first-order critical speed, but the oil film whip occurred when it was accelerated to 3000 rpm, and the amplitude began to increase sharply. From the theoretical analysis of the fourth part, it is known that when the ellipticity is 0.7, the rotor system has a half-frequency whirl across the critical speed. This is a precursor to oil film instability. When the rotational speed reaches twice the critical speed, the half-frequency whirl frequency and the critical speed are equal, causing a strong resonance, resulting in instability of the rotor system. These experimental phenomena are consistent with the previous theoretical analysis results, verifying the correctness of theoretical analysis.

In order to eliminate the oil film whip during the second acceleration, the ellipticity is adjusted at the 23rd second to reduce the working position of the journal, see Fig. 15. The second acceleration process is the same as the condition of the first acceleration process. The only difference is that the bearing ellipticity is adjusted after the critical speed is reached. In the test, the oil film whip appeared after the rotor was accelerated to 3000 rpm, and the amplitude began to increase. However, after adjusting the ellipticity at the 23rd second, the working position of the

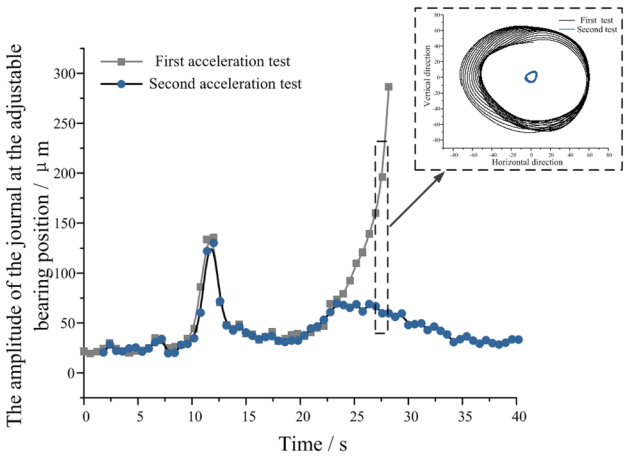


**Fig. 16** Comparison of vibration of rotor during two acceleration processes

journal in the bearing pad was lowered and the amplitude began to decrease. At 32 s, the amplitude of the journal has been reduced to a stable operating state. From the phenomenon in the second experiment, it can be proved that the oil film whip can be eliminated by reducing the ellipticity to reduce the working position of the rotor.

The experimental data of the two acceleration processes were used to plot the journal amplitude variation curve, see Fig. 16. The vibrations of the two experiments were completely consistent before accelerating to 3000 rpm. After reaching 3000 rpm, the first experiment did not adjust the ellipticity, and the amplitude of the rotor began to increase sharply. Extracting the experimental data of 27 s to draw the axis orbit found that there is oil film whip, which seriously affects the safe and stable operation of the rotor system. In the second experiment, the ellipticity was adjusted from 0.7 to 0.2 at the 23rd second, the vibration of the rotor was significantly reduced, and it was quickly restored to a stable working state. The 27th second experimental data was extracted to draw the axis orbit, and it was found that the oil film whip had been eliminated. Through these two comparison experiments, it can be concluded that reducing the ellipticity can eliminate the oil film whip and improve the stability of the rotor system. This prove that the adjustable bearing can establish a better stability mechanism of the rotor system.

## 6 Conclusions

This paper proposes a new type of adjustable bearing that has the ability to change the lubrication properties of the bearing. This kind of adjustable bearing is more suitable for the changing working conditions than traditional fixed-bearing bearings. During the operation of rotating machinery, the stability and reliability of the rotating machinery can be significantly improved by specifying reasonable control strategy and selecting reasonable oil film thickness for different working conditions.

Firstly, the working principle of the adjustable bearing is introduced. Then, the evaluation method of the dynamic characteristics of the adjustable bearing is established. Finally, the dynamic response of the rotor system is solved by Runge–Kutta variable step integral. Based on the results and discussions, the following conclusions are drawn:

a. During the acceleration process, the vibration of the journal can be reduced by increasing the ellipticity. However, in this case, the half-frequency whirl frequency occurs when the rotational speed exceeds the critical speed. This indicates a safety hazard in the rotor system. The correct adjustment method is to reduce the ellipticity and increase the oil film gap when the critical speed is exceeded, thereby improving the stability of the rotor system.
b. When the oil film whip occurs in the rotor system, the ellipticity is adjusted to reduce the working position of the rotor in the bearing pad, which can suppress the problem of oil film whip. Two comparison experiments verify that the adjustable bearing can establish a better rotor system stability mechanism and improve the stability of the rotating machine.
c. This adjustable bearing structure achieves the function of changing the characteristic parameters of the bearing under a continuous operation. A reasonable adjustment of the ellipticity can effectively improve the stability of the rotor system.

Current research has achieved a manual adjustment of bearing parameters. When the amplitude of the journal starts to increase, the vibration of the journal is reduced by manually adjusting the ellipticity to improve the stability of the rotor system. Future research plan is that the adjustable bearing has the ability to automatically adjust the bearing's characteristic parameters using a time–frequency controller to actively regulate the adjustable bearing. At present, nonlinear time–frequency controllers are being developed and subsequent non-linear time–frequency control methods will be used to achieve active control of adjustable bearings.

**Acknowledgements** This study was funded by the project of National Natural Science Foundation of China (Grant No. 51575421).

## Compliance with ethical standards

**Conflict of interest** The authors declare that they have no conflict of interest.

## References


1. Rao JS, Tiwari R (2006). Design optimization of thrust magnetic bearings using genetic algorithms. In: Seventh IFToMM-conference on rotor dynamics, Vienna, Austria, vol 1, pp 25–28
2. Rao JS, Tiwari R (2008) Optimum design & analysis of thrust magnetic bearings using multi objective genetic algorithms. Int J Comput Methods Eng Sci Mech 9(4):223–245
3. Dohnal F, Markert R (2011) Enhancement of external damping of a flexible rotor in active magnetic bearings by time-periodic stiffness variation. J Syst Dyn 5:856–865
4. Palazzolo AB, Lin RR, Alexander RM, Kascak AF, Montague J (1991) Test and theory for piezoelectric actuator for active vibration control of rotating machinery. ASME J Vib Acoust 113:167–175
5. Tuma J, Simek J, Skuta J, Los J (2013) Active vibrations control of journal bearings with the use of piezoactuators. Mech Syst Signal Process 36:618–629
6. Ishida Y, Liu J (2008) Vibration suppression of rotating machinery utilizing discontinuous spring characteristics. ASME J Vibr Acoust 130(3):03100
7. Santos IF (1994) Design and evaluation of two types of active tilting-pad journal bearings. In: Proceedings of the IUTAM symposium on active control of vibration, Bath, England, Kluwer, Dordreicht, The Netherlands, pp 79–87
8. Santos IF, Scalabrin A (2000) Control system design for active lubrication with theoretical and experimental examples, ASME Paper No. 2000-GT-643
9. Nicoletti R, Santos IF (2001) Vibration control of rotating machinery using active tilting-pad bearings. In: Proceedings of the IEEE/ASME international conference on advanced intelligent mechatronics, Como, Italy, July 8–11, pp 589–594
10. Santos IF, Nicoletti R (2001) Influence of orifice distribution on the thermal and static properties of hybridly lubricated bearings. Int J Solids Struct 38(10–13):2069–2081
11. Krodkiewski JM, Sun L (1988) Modelling of multi-bearing rotor system incorporating an active journal bearing. J Sound Vib 210:215–229
12. Krodkiewski JM, Cen Y, Sun L (1997) Improvement of stability of rotor system by introducing a hydrodynamic damper into an active journal bearing. Int J Rotor Mach 3:45–52
13. Sun L, Krodkiewski JM, Cen Y (1988) Self-tuning adaptive control of forced vibration in rotor system using an active journal bearing. J Sound Vib 213:1–14
14. Chasalevris A, Dohnal F (2012) A journal bearing with variable geometry for the reduction of the maximum response amplitude during passage through resonance. ASME J Vib Acoust 134:061005
15. Chasalevris A, Dohnal F (2014) Vibration quenching in a large scale rotor-bearing system using journal bearings with variable geometry. J Sound Vib 333:2087–2099
16. Chasalevris A, Dohnal F (2015) A journal bearing with variable geometry for the suppression of vibrations in rotating shafts: simulation, design, construction and experiment. Mech Syst Signal Proc 52–53:506–528
17. Chasalevris A, Dohnal F (2016) Improving stability and operation of turbine rotors using adjustable journal bearings. Tribol Int 104:369–382
18. Sivrioglu AS (2007) Adaptive control of nonlinear zero-bias current magnetic bearing system. Nonlinear Dyn 48:175–184
19. Iwada Y, Nonami K (1983) Vibration control of rotating shaft with self-optimizing support system. Trans JSME 49:1897–1903 **in Japanese**
20. Reinig KD, Desrochers AA (1986) Disturbance accommodating controllers for rotating mechanical system. ASME J Dyn Syst Meas Control 108:24–31